

PAPER • OPEN ACCESS

## Analysis and improvement of self-heating effect based on GaN HEMT devices

To cite this article: Zhipeng Zuo *et al* 2022 *Mater. Res. Express* **9** 075903

View the [article online](#) for updates and enhancements.

### You may also like

- [Inferring the Neutron Star Maximum Mass and Lower Mass Gap in Neutron Star-Black Hole Systems with Spin](#)  
Christine Ye and Maya Fishbach
- [Analysis on accumulated deformation and stress of the steel roof of Beijing Opera House during construction](#)  
L L Wu, G Gao, B R Ye *et al.*
- [Research on steel bridge deck pavement mechanical response of Urumqi express way](#)  
M Zhang, Z D Qian, Y C Xue *et al.*



The Electrochemical Society  
Advancing solid state & electrochemical science & technology

# UNITED THROUGH SCIENCE & TECHNOLOGY

**248th  
ECS Meeting**  
Chicago, IL  
October 12-16, 2025  
*Hilton Chicago*



**Science +  
Technology +  
YOU!**

**SUBMIT  
ABSTRACTS by  
March 28, 2025**

**SUBMIT NOW**

# Materials Research Express



## PAPER

### OPEN ACCESS

RECEIVED  
26 May 2022

REVISED  
9 July 2022

ACCEPTED FOR PUBLICATION  
20 July 2022

PUBLISHED  
27 July 2022

Original content from this work may be used under the terms of the [Creative Commons Attribution 4.0 licence](#).

Any further distribution of this work must maintain attribution to the author(s) and the title of the work, journal citation and DOI.



# Analysis and improvement of self-heating effect based on GaN HEMT devices

Zhipeng Zuo\*, Naiyun Tang and Hui Chen

Shanghai University of Electric Power, School of Electronics and Information Engineering, 200000, Shanghai, People's Republic of China

\* Author to whom any correspondence should be addressed.

E-mail: [1427523733@qq.com](mailto:1427523733@qq.com)

**Keywords:** GaN HEMT, self-heating effect, current collapse

## Abstract

Gallium nitride high electron mobility transistor (GaN HEMT) applications in high-power and high-frequency environments can lead to high device temperatures due to the self-heating effect, thus limiting device performance and reliability. In order to address this problem, this paper changes the material and structure of the device. It successfully reduces the maximum temperature of the device to 335 K by using a new structure of the diamond substrate, diamond heat sink layer, and InGaN insertion layer. Simulation results show that the new structure has a 35% reduction in maximum temperature, a 61% increase in current, a 37% improvement in maximum transconductance, and a 35% improvement in current collapse. At the same time, the new structure also improves the electron mobility of the channel.

## 1. Introduction

GaN HEMT devices are gaining attention in microwave and high-power applications due to their high thermal conductivity, wideband gaps, high breakdown voltages, and high electron mobility [1–3]. However, the increased channel temperature during the operation of GaN HEMT devices can cause problems such as self-heating and current collapse [4, 5]. Sapphire and silicon are traditional substrates for GaN HEMT devices. The low thermal conductivity of sapphire and silicon makes it difficult to dissipate heat, aggravating GaN HEMT devices' self-heating tendency. Therefore, choosing a material with high thermal conductivity for the substrate can increase the device's thermal capability and reduce its self-heating effect. The thermal conductivity of diamond at room temperature is  $2000 \text{ W} \cdot \text{m}^{-1} \cdot \text{K}^{-1}$  and its heat dissipation effect is considerable [6, 7]. Currently, GaN HEMT can be integrated with the diamond in two ways: one is by removing the substrate and replacing it with diamond [8, 9]; the other is by growing diamond directly onto the device channel using chemical vapour deposition [10, 11]. M. Malakoutian *et al* have demonstrated by I-V thermometry that integrating diamond in GaN devices can reduce the device channel temperature [12]. Passivating layers like  $\text{Si}_3\text{N}_4$  suppress current collapse, but poor thermal conductivity ( $10 \text{ W} \cdot \text{m}^{-1} \cdot \text{K}^{-1}$ ) prevents heat from dissipating [13]. Using different passivation layer materials can reduce the self-heating effect of GaN HEMT devices [14–16]. To reduce the self-heating effect and suppress current collapse, researchers have explored using AlN ( $285 \text{ W} \cdot \text{m}^{-1} \cdot \text{K}^{-1}$ ) as a passivation layer [17]. However, the heat dissipation effect of AlN is limited, which is not conducive to the further improvement of device performance.

This paper uses Silvaco TCAD software to simulate the GaN HEMT device and analyzes the self-heating effect and current collapse. By changing the material and structure of the GaN HEMT, the channel's temperature is reduced, effectively reducing the self-heating effect and suppressing the current collapse, improving the performance and reliability of the device.

## 2. Device structures and simulation models

The device structure of a conventional GaN HEMT is shown in figure 1, with a device length of  $4.5 \mu\text{m}$ , a height of  $5.35 \mu\text{m}$ , and a width of  $100 \mu\text{m}$ . The length of source is  $0.5 \mu\text{m}$ , and the length of drain is  $1.5 \mu\text{m}$ , both of

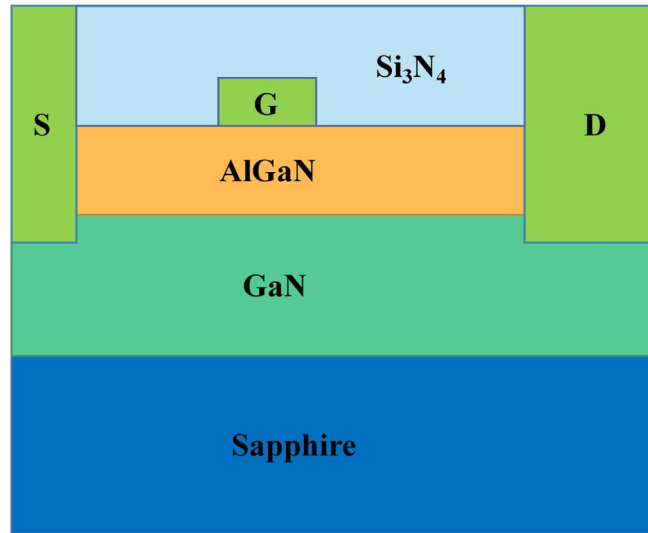


**Figure 1.** Structure of conventional GaN HEMT device.

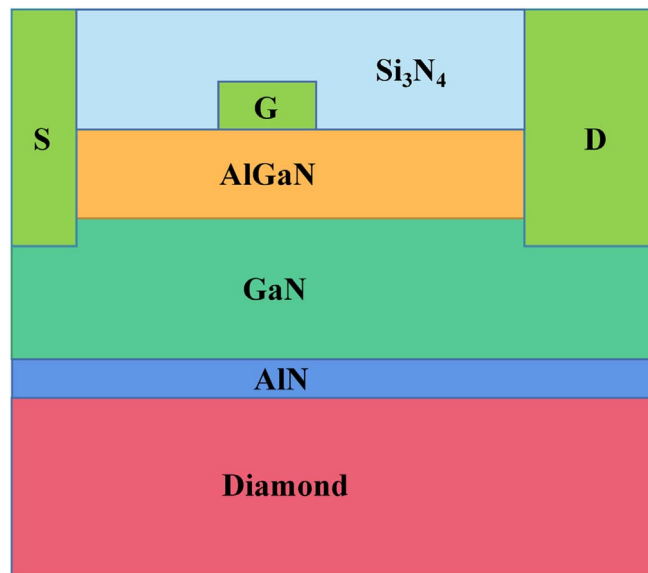


**Figure 2.** Device structure on the diamond substrate.

which have a thickness of  $0.37 \mu\text{m}$ . The length of gate is  $0.4 \mu\text{m}$ , and the thickness is  $0.09 \mu\text{m}$ . In addition, the gate-source pitch is  $0.93 \mu\text{m}$ , and the gate-drain pitch is  $1.17 \mu\text{m}$ . The source and drain are ohmic contacts, and the gate is a Schottky contact with a work function of  $5.1 \text{ eV}$ . The length of  $\text{Si}_3\text{N}_4$  is  $2.5 \mu\text{m}$ , and the thickness is  $0.325 \mu\text{m}$ . The length of  $\text{Al}_{0.26}\text{Ga}_{0.74}\text{N}$  is  $2.5 \mu\text{m}$ , and the thickness is  $0.025 \mu\text{m}$ . The thickness of GaN is  $2.3 \mu\text{m}$ , and the thickness of sapphire is  $2.7 \mu\text{m}$ . Figure 2 shows the device structure of the diamond substrate with a diamond thickness of  $2.7 \mu\text{m}$ . In order to reduce the lattice mismatch between diamond and GaN, the thickness of inserted AlN is  $0.3 \mu\text{m}$ , and the rest parameters are the same as in figure 1. Figure 3 shows the device structure with diamond and AlN as the heat sink layer based on figure 2. The thickness of the diamond is  $1.88 \mu\text{m}$ , and the thickness of AlN is  $0.144 \mu\text{m}$ . The length of the GaN bubble layer below the gate is  $2.5 \mu\text{m}$ , and the thickness is  $1 \text{ nm}$ . In addition, the doping concentration is  $1 \times 10^{20} \text{ cm}^{-3}$ , and the doping type is n-type. Figure 4 shows the device structure of the  $\text{In}_{0.15}\text{Ga}_{0.85}\text{N}$  insertion layer with a length of  $1.1 \mu\text{m}$  and a thickness of  $2 \text{ nm}$ .

In this paper, the device is simulated using various models of Silvaco TCAD software. The generation and recombination of carriers are related to temperature. Therefore, the simulation adopts the SRH model. GaN HEMT devices generate the self-heating effect during operation, and the heat of the channel will be transferred to other locations through heat transfer. Therefore, the lattice heat transfer model and heat generation model are

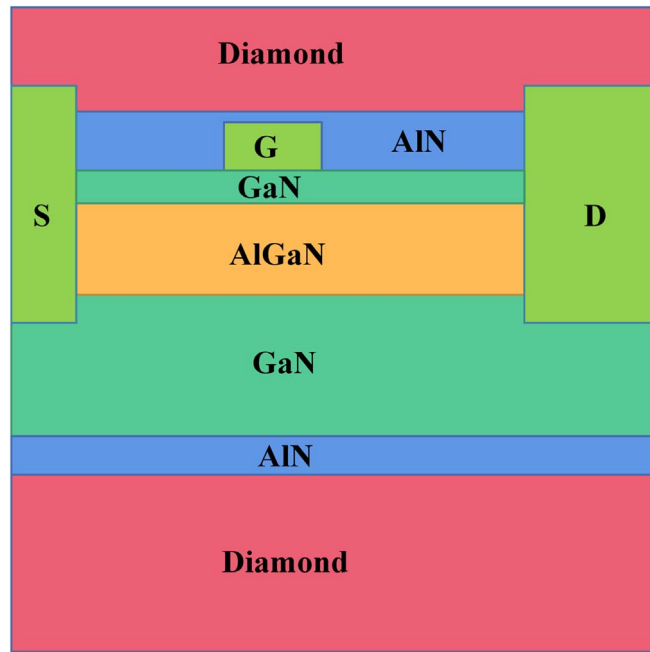


**Figure 3.** The device structure of the diamond heat sink layer.

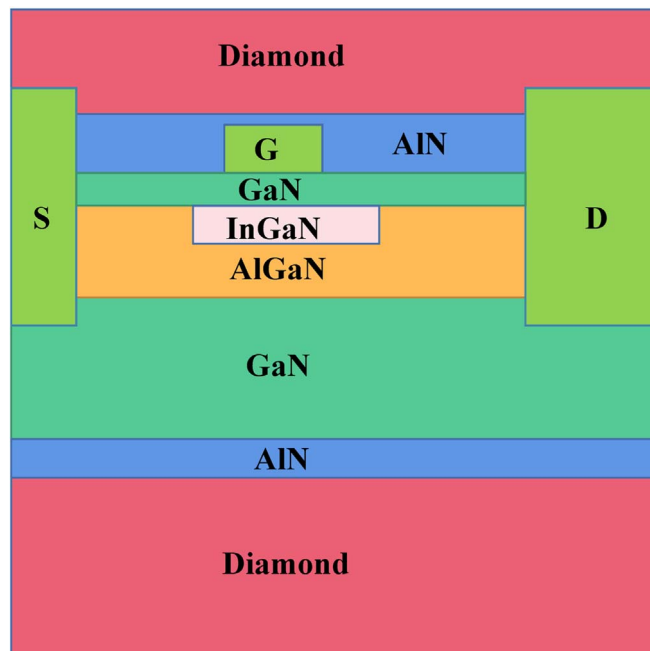


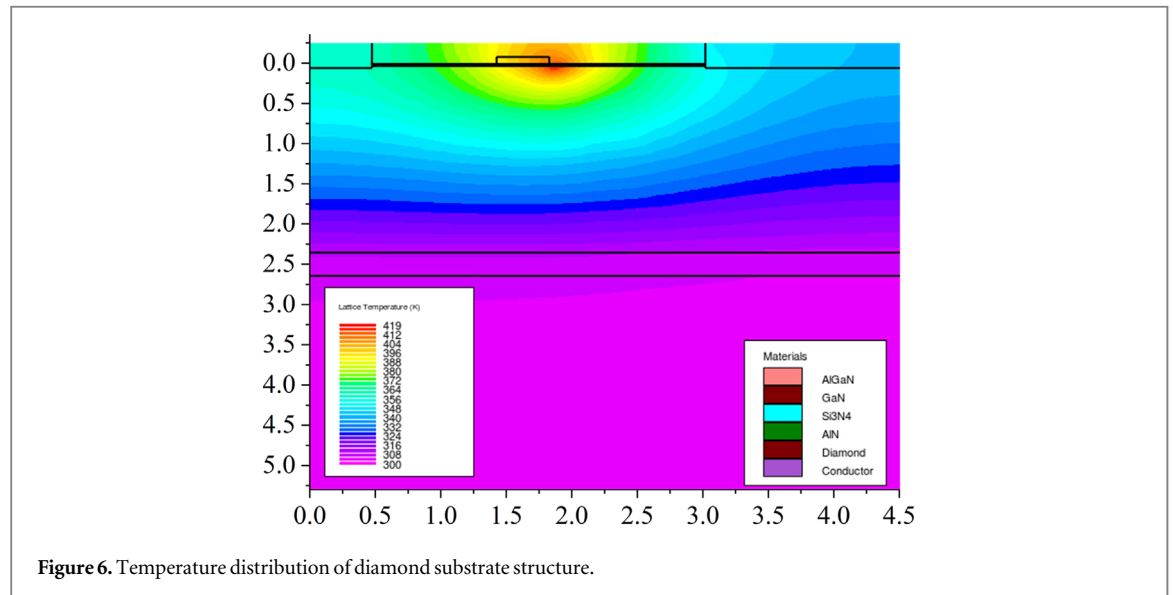
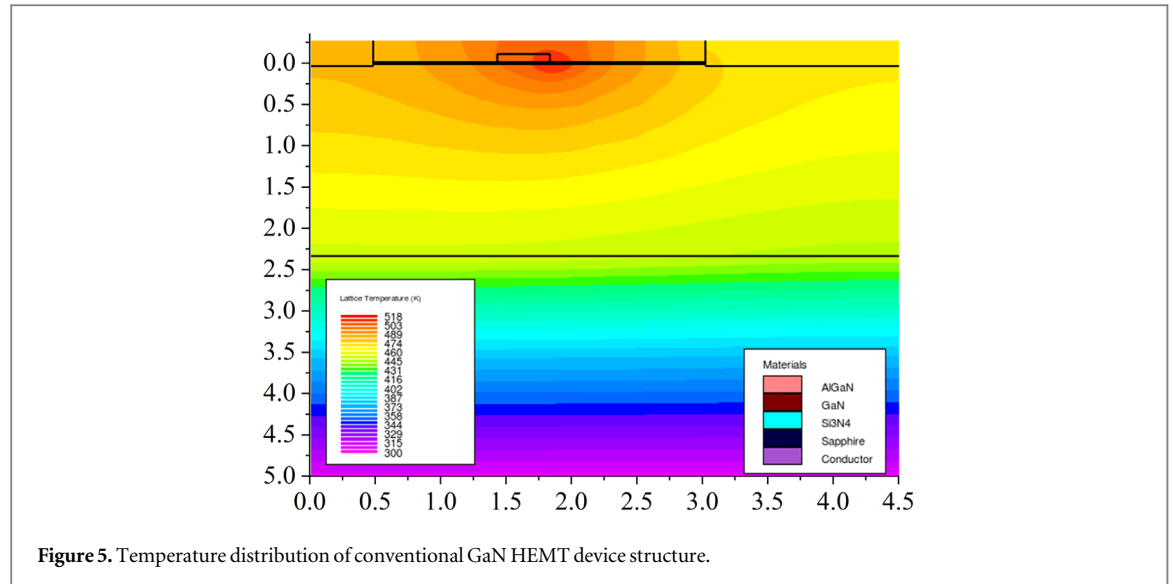
**Figure 4.** The device structure of the InGaIn insertion layer.

required. GaN HEMT devices have different thermal conductivity coefficients for each material layer. Therefore, the material thermal conductivity model needs to be used. At the same time, the mobility model and polarization model are also used in the simulation.

### 3. Results and discussion

#### 3.1. Effects of diamond substrate on device characteristics

Figure 5 shows the temperature distribution of the conventional GaN HEMT device structure, and figure 6 shows the temperature distribution of the diamond substrate structure. As can be seen from the figure, the



highest temperature of the device is near the channel, which is mainly due to the high electrons concentration in the channel. When electrons flow from the source to the drain under the action of an electric field, various scattering will occur, causing the temperature of the device to increase, among which lattice scattering plays a significant role. The increase of temperature will enhance the scattering, and the enhancement of scattering will intensify the increase of temperature, resulting in the decrease of carrier mobility. The maximum temperature of conventional GaN HEMT device structures is 518 K when  $V_{GS} = 0$  V and  $V_{DS} = 15$  V, and there is a wide range of high-temperature regions. This is mainly due to the low thermal conductivity of sapphire, which is not conducive to the heat dissipation of the device. When the diamond is used as the substrate, the high-temperature region of the device shrinks rapidly, and the maximum temperature drops to 419 K. The lattice scattering effect is weakened, and the electron mobility of the channel increases. Figure 7 shows the conventional and diamond substrate structure's channel temperature distribution curves. From the figure, it can be observed that the temperature curve of the diamond substrate structure is entirely below the temperature curve of the traditional structure. The use of diamond material as a substrate affects the device's current and lowers the temperature. Figure 8 shows the output curves of the conventional structure and the diamond substrate structure. From the figure, it can be seen that the peak value of the current increases from  $0.85 \text{ A mm}^{-1}$  to  $1.2 \text{ A mm}^{-1}$ . However, the currents of both drop rapidly with the increase of drain voltage after reaching the peak, and the current collapse occurs. When  $V_{GS} = 0$  V, a linear approximation is made to the saturated part of the output curve of the conventional structure, which has a current collapse rate of 35%, while that of the diamond substrate structure is 18.5%.

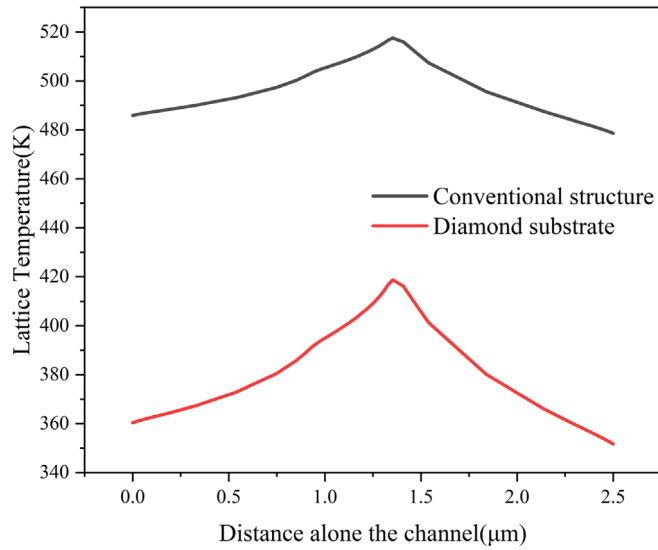


Figure 7. Channel temperature distribution curves for conventional and diamond substrate structures.

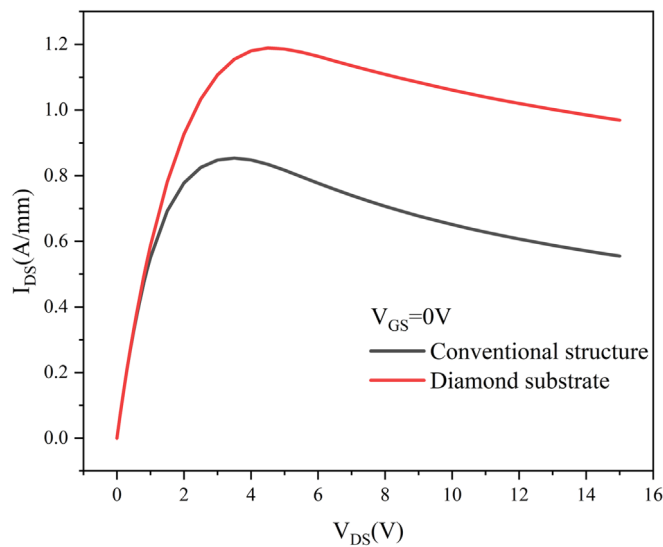


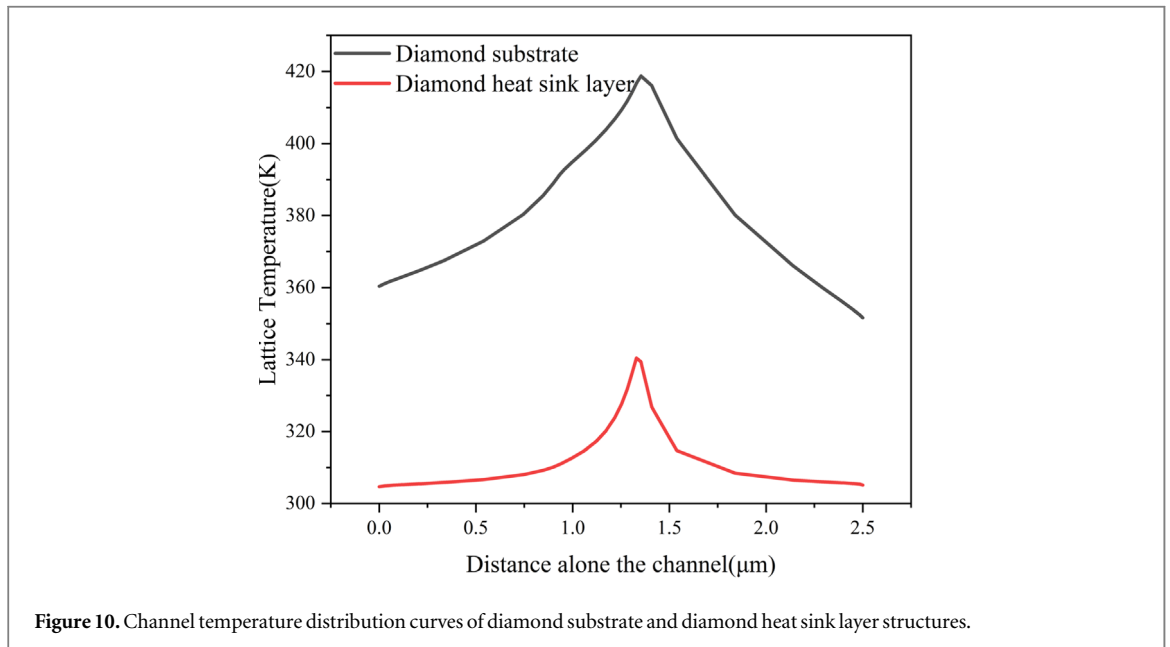
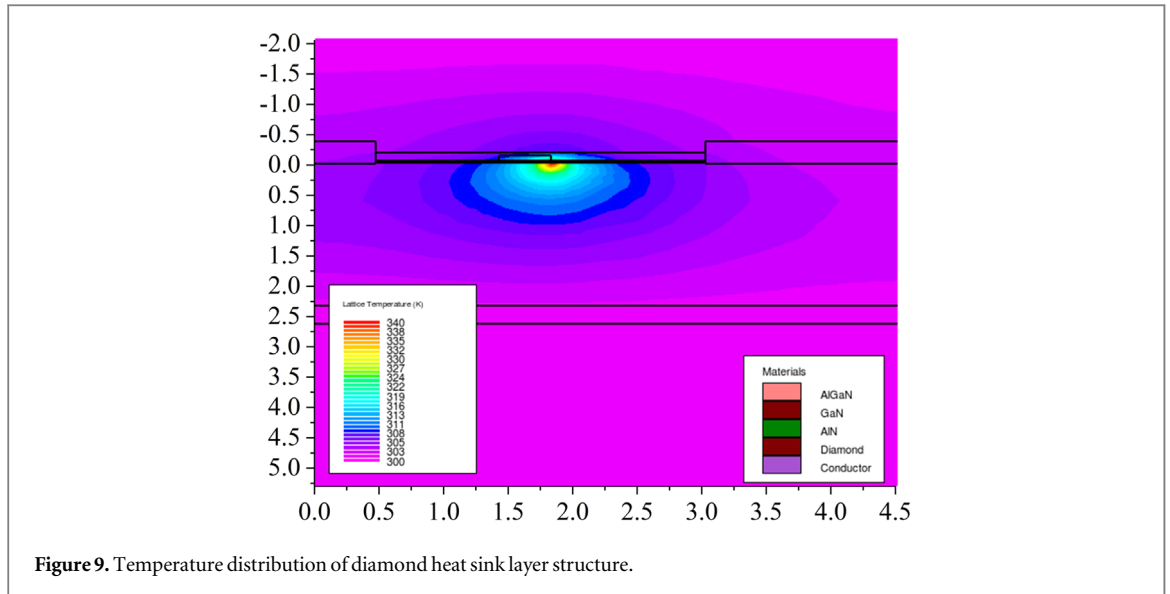
Figure 8. Output curves for conventional and diamond substrate structures.

### 3.2. Effects of diamond heat sink layer on device characteristics

The most common passivation layer used in traditional GaN HEMT device structure is  $\text{Si}_3\text{N}_4$ . However, the poor thermal conductivity of  $\text{Si}_3\text{N}_4$  limits the further heat dissipation of GaN HEMT devices. Figure 9 shows the temperature distribution of the diamond heat sink layer structure, and figure 10 shows the channel temperature distribution curves of the diamond substrate and the diamond heat sink layer structures. After using diamond as the heat sink layer, the channel temperature can be dissipated from the bottom and top of the device at the same time, and the peak temperature is reduced from 419 K to 340 K. In addition, the distribution curve of channel temperature is all lower than the original curve.

Figure 11 shows the output curves of diamond substrate and diamond heat sink layer structures. In addition, the output curve of the diamond substrate structure shows a serious current collapse. With the use of diamond as the heat sink layer, the output current remains constant as the drain voltage increases, significantly suppressing current collapse. Some research groups have found that the trap captured electrons on the device surface with the potential barrier and buffer layers are the microscopic cause of current collapse [18, 19]. As the temperature decreases, it becomes more and more difficult for traps on the device surface to trap electrons in the barrier and buffer layers, thereby suppressing current collapse. On the other hand, the current collapse is suppressed by weakening lattice scattering. When using conventional  $\text{Si}_3\text{N}_4$  as the passivation layer, the





maximum temperature of the device is 419 K. The higher the temperature, the higher the energy of the carrier and the greater the probability of lattice scattering. Therefore, the stronger the effect of lattice scattering. As the drain voltage increases, the device temperature rises, leading to enhanced lattice scattering, resulting in a rapid drop in output current. The use of diamond as a heat sink layer reduces the maximum device temperature to 340 K. The reduction in temperature significantly suppresses lattice scattering and current collapse.

### 3.3. Effects of InGaIn insertion layer on device characteristics

In order to further reduce the device temperature, a new structure of the InGaIn insertion layer is proposed in this paper, and its structure is shown in figure 4. Since the peak of the device temperature is near the gate, it can be considered to insert a thin layer of InGaIn into the AlGaIn to reduce the temperature of the device. The InGaIn insertion layer is introduced to induce polarized negative charges from the heterojunction of the InGaIn insertion layer and AlGaIn barrier layer. The polarized negative charges decrease the electrons concentration in the two-dimensional electron gas. In this way, the device temperature can be reduced. The temperature distribution of the InGaIn insertion layer structure is shown in figure 12. Figure 13 shows the channel temperature distribution curves of the diamond heat sink layer and the InGaIn insertion layer structures. The peak of device temperature is further reduced to 335 K after the insertion of InGaIn in AlGaIn. From the figure, it can be seen that the channel temperature curve of the InGaIn insertion layer structure is almost entirely below

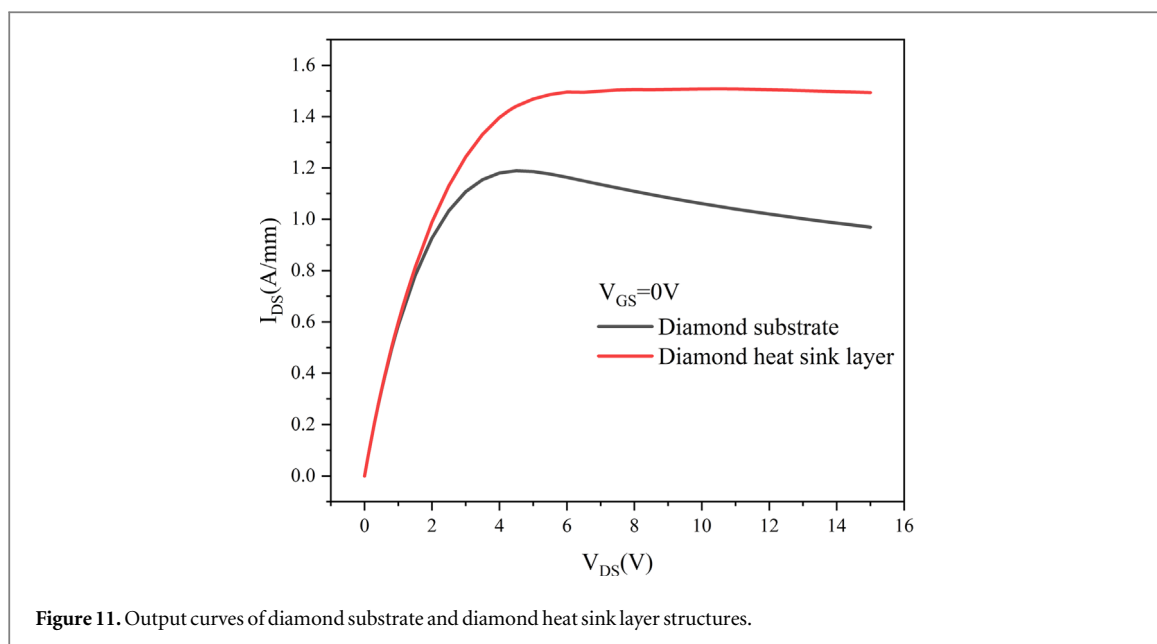


**Figure 11.** Output curves of diamond substrate and diamond heat sink layer structures.

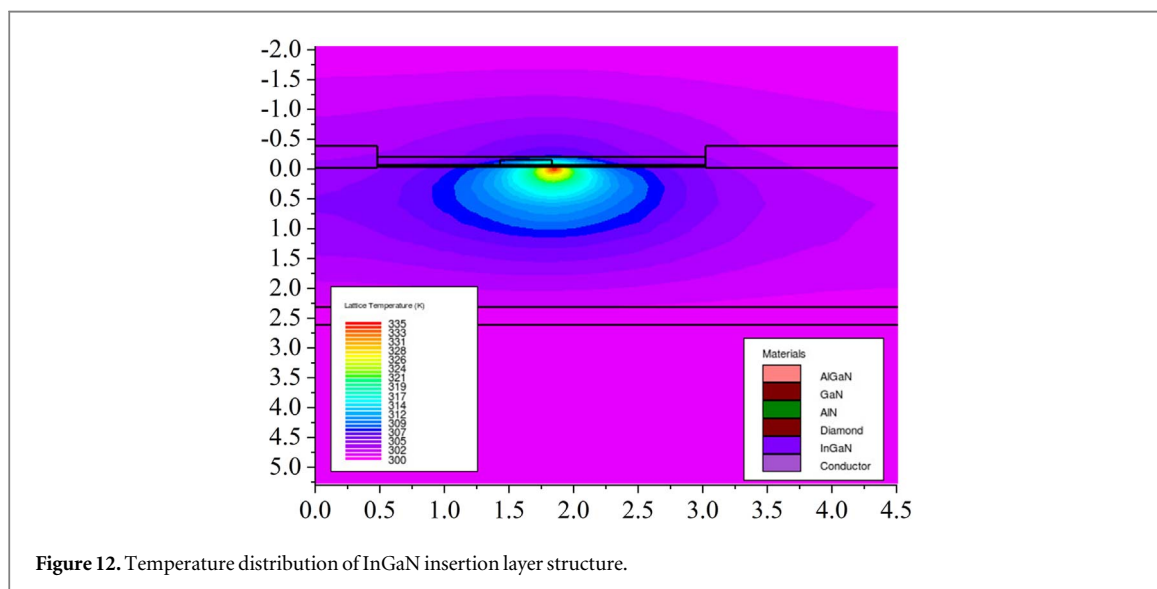


**Figure 12.** Temperature distribution of InGaN insertion layer structure.

the channel temperature distribution curve of the diamond heat sink layer structure, and its maximum temperature is lower than the maximum temperature of the diamond heat sink layer structure. Therefore, there is no diffusion in the high-temperature region of the InGaN insertion layer structure compared to the diamond heat sink layer structure. Output curves of the diamond heat sink layer and InGaN insertion layer structures are shown in figure 14. The structure of the InGaN insertion layer improves current collapse by 35% compared to conventional structures. The polarized negative charges are induced in the heterojunction of the InGaN insertion layer and AlGaN barrier layer. The polarized negative charges decrease the electrons concentration in the two-dimensional electron gas, resulting in a lower drain current. As a result, the temperature of the device is reduced. Figure 15 shows the transient curves of the traditional structure and the InGaN intercalation layer structure. The device with the traditional structure will seriously reduce the electron mobility in the channel due to the high temperature. As a result, its transient curve decreases rapidly after reaching its peak and reaches a steady-state current value that is severely below the peak. InGaN insertion layer structure has a lower device temperature, which reduces lattice scattering and significantly increases electron mobility in the channel. Therefore, its transient curve does not decrease rapidly after reaching the peak, showing excellent switching characteristics. Figure 16 shows the transconductance curves of the traditional structure and the InGaN intercalation layer structure. It can be seen that the transconductance of the InGaN intercalation layer structure has been dramatically improved compared with that of the traditional structure. The peak transconductance of



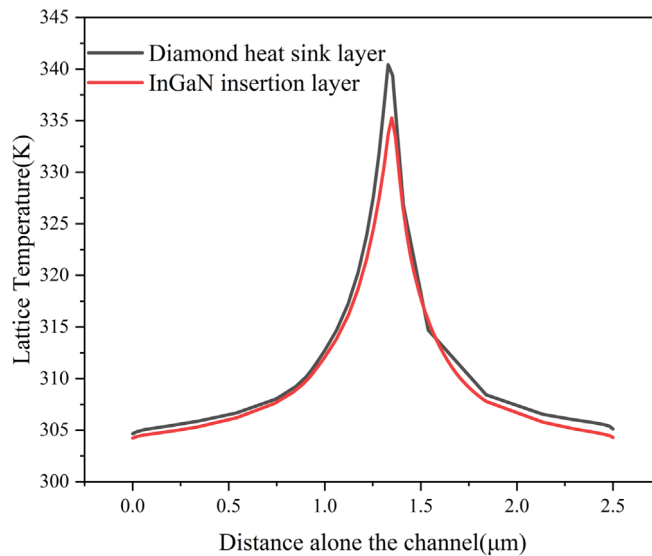


**Figure 13.** Channel temperature distribution curves of diamond heat sink layer and InGaN insertion layer structures.

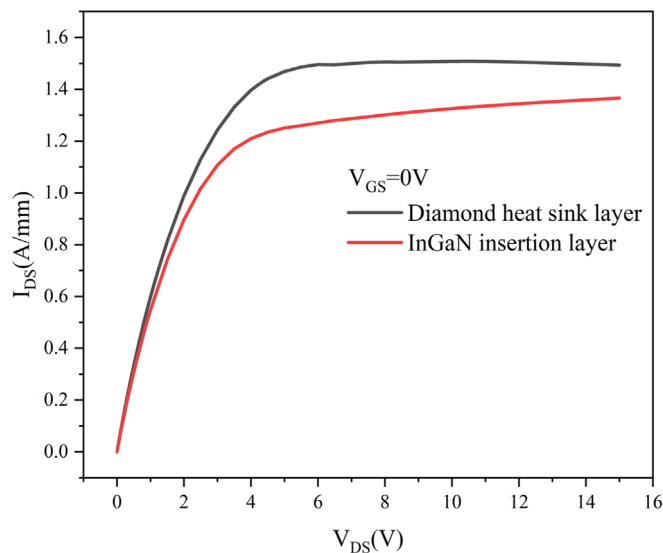


**Figure 14.** Output curves of diamond heat sink layer and InGaN insertion layer structures.

the conventional structure is  $240 \text{ mS mm}^{-1}$ , and the peak transconductance of the InGaN insertion layer structure is  $329 \text{ mS mm}^{-1}$ , which increases the maximum transconductance by 37% in comparison.

#### 4. Conclusion

In high power transistors, the excessive temperature of GaN HEMT devices significantly limits their performance. In this paper, starting from the traditional GaN HEMT device structure, the thermal simulation of the device is carried out by changing the material and structure of the device. By using a diamond substrate, a new structure of the diamond heat dissipation layer and the InGaN intercalation layer successfully reduces the temperature of the device and increases the electron mobility of the channel. The maximum temperature of the device is reduced from 518 K to 335 K, a 35% temperature reduction. The output current is increased from  $0.85 \text{ A mm}^{-1}$  to  $1.37 \text{ A mm}^{-1}$ , a 61% increase in output current and a 35% improvement in current collapse. At the same time, the maximum transconductance of the device increases from  $240 \text{ mS mm}^{-1}$  to  $329 \text{ mS mm}^{-1}$ , an increase of 37%. Therefore, the structure of this paper improves the electrical characteristics of GaN HEMT

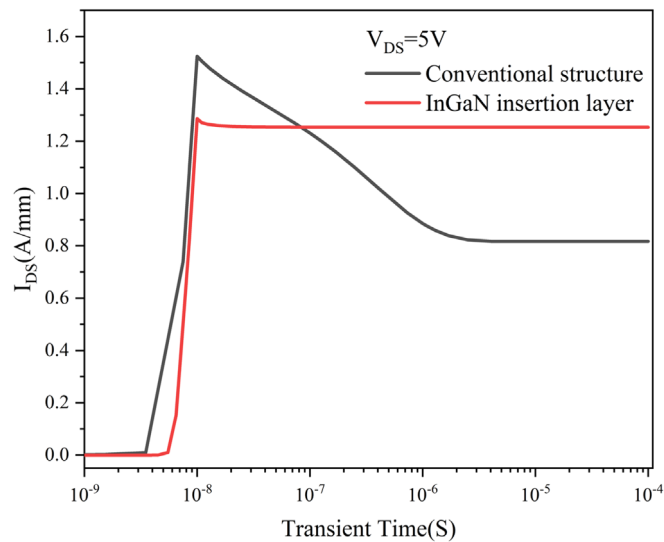


**Figure 15.** Transient curves of conventional structure and InGaN insertion layer structure.

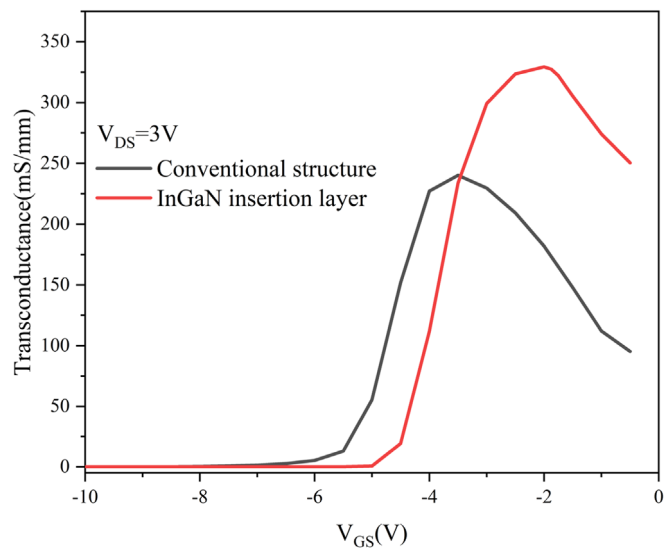


**Figure 16.** Transconductance curves of conventional structure and InGaN intercalation layer structure.

devices and enhances the reliability of operation. At the same time, this paper has some merits in researching the self-heating effect and current collapse of GaN HEMT devices.

### Data availability statement

All data that support the findings of this study are included within the article (and any supplementary files).

### ORCID iDs

Zhipeng Zuo  <https://orcid.org/0000-0003-3340-7416>

### References

- [1] Jarndal A H and Bassal A M 2019 A broadband hybrid GaN cascode low noise amplifier for WiMax applications *Int. J. RfMicrow. C. E.* **29** e21456
- [2] Jarndal A et al 2020 Reliable noise modeling of GaN HEMTs for designing low-noise amplifiers *Int. J. Numer. Model. El.* **33** e2585

- [3] Liu J *et al* 2020 Analytical model for the potential and electric field distributions of AlGaIn/GaN HEMTs with gate-connected FP based on equivalent potential method *Superlattice. Microst.* **138** 106327
- [4] Chatterjee B *et al* 2020 Nanoscale electro-thermal interactions in AlGaIn/GaN high electron mobility transistors *J. Appl. Phys.* **127** 044502
- [5] Chandrasekar H *et al* 2018 Buffer-induced current collapse in GaN HEMTs on highly resistive Si substrates *IEEE Electr Device L.* **39** 1556
- [6] Anaya J *et al* 2016 Control of the in-plane thermal conductivity of ultra-thin nanocrystalline diamond films through the grain and grain boundary properties *Acta Mater.* **103** 141–52
- [7] Xu R L *et al* 2019 Thermal conductivity of crystalline AlN and the influence of atomic-scale defects *J. Appl. Phys.* **126** 185105
- [8] Ohki T *et al* 2018 An over 20-W/mm S-band InAlGaIn/GaN HEMT with SiC/diamond-bonded heat spreader *IEEE Electr. Device L.* **40** 287–90
- [9] Dumka D C *et al* 2013 Electrical and thermal performance of AlGaIn/GaN HEMTs on diamond substrate for RF applications, IEEE Compound semiconductor integrated circuit symposium (CSICS) *IEEE* **2013** 1–4
- [10] Laurent M A, Malakoutian M and Chowdhury S 2019 A study on the nucleation and MPCVD growth of thin, dense, and contiguous nanocrystalline diamond films on bare and Si<sub>3</sub>N<sub>4</sub>-coated N-polar GaN *Semicond. Sci. Tech.* **35** 015003
- [11] Malakoutian M, Laurent M A and Chowdhury S 2019 A study on the growth window of polycrystalline diamond on Si<sub>3</sub>N<sub>4</sub>-coated N-polar GaN *Crystals* **9** 498
- [12] Malakoutian M *et al* 2021 Development of polycrystalline diamond compatible with the latest N-polar GaN mm-wave technology *Cryst. Growth Des.* **21** 2624–32
- [13] Whiteside M *et al* 2020 Improved interface state density by low temperature epitaxy grown AlN for AlGaIn/GaN metal-insulator-semiconductor diodes *mater Sci. Eng. B-Adv.* **262** 114707
- [14] Haghshenas A, Fathipour M and Mojab A 2011 Dependence of self-heating effect on passivation layer in AlGaIn/GaN HEMT devices, international semiconductor device research symposium (ISDRS) *IEEE* **2011** 1–2
- [15] Chander S *et al* 2020 Self-heating effects in gan high electron mobility transistor for different passivation material *Defence Sci. J.* **70** 511–4
- [16] Arivazhagan L *et al* 2021 A numerical investigation of heat suppression in HEMT for power electronics application *Silicon-Neth* **13** 3039–46
- [17] Tsurumi N *et al* 2010 AlN passivation over AlGaIn/GaN HFETs for surface heat spreading *IEEE T. Electron Dev* **57** 980–5
- [18] Zhang Y *et al* 2014 Effect of self-heating on the drain current transient response in AlGaIn/GaN HEMTs *IEEE Electr. Device L.* **35** 345–7
- [19] Wang A *et al* 2014 Simulation of temperature and electric field-dependent barrier traps effects in AlGaIn/GaN HEMTs *Semicond. Sci. Tech.* **30** 015010